Meso Scale Discovery®
A division of Meso Scale Diagnostics, LLC.
www.mesoscale.com®

Evaluation of the Circulating Angiome in Cancer: Translational Assessment of a 44-Plex Angiogenesis Biomarker Panel

Hans Layman[1], Mai Abdel-Ghani[1], David Cheo[1], Marco Morelli[1], Grace Galen[1], Marisela Arana[1], Anu Mathew[1], Mingyue Wang[1], Catherine Demos[1], Jack Smith[1], Brian Ngo[1], Nicholas Sammons[1], Nikhil Padmanabhan[1], Pankaj Oberoi[1], Andrew B. Nixon[2], Jacob N. Wohlstadter[1]

[1]Meso Scale Diagnostics, LLC., Rockville, MD, USA, [2]Duke University, Durham, NC, USA

Introduction

Angiogenesis is a hallmark of tumor progression. Dysregulated angiogenesis in the tumor microenvironment leads to leaky, poorly perfused vessels, hypoxia, immune evasion, and therapeutic resistance. Despite widespread use of anti-angiogenic agents, no predictive biomarker identifies likely responders. Prior biomarker efforts focused on limited vascular factors, missing the multifaceted nature of angiogenic signaling. MSD developed a 44-plex panel to enable high-throughput profiling of pro- and anti-angiogenic biomarkers addressing key stages of angiogenesis (Figure 1).

1. Hypoxic Insult: Tumor hypoxia stabilizes HIF signaling, inducing secretion of pro-angiogenic growth factors (e.g., VEGF-A, VEGF-C, PlGF, HGF, Ang-2) that initiate vascular remodeling and endothelial activation.
2. Basement Membrane Degradation: Proteolytic remodeling of the extracellular matrix enables endothelial cell invasion, mediated by enzymes such as MMP-2, MMP-9 (active) and matrix-associated proteins including Osteopontin and Pentraxin-3.
3. Tip Cell Migration: Chemokine-driven guidance of endothelial tip cells directs sprouting toward angiogenic signals, with key mediators including SDF-1α (CXCL12), MCP-1 (CCL2), Fractalkine (CX3CL1), MIG (CXCL9), and IP-10 (CXCL10).
4. Tube Formation: Endothelial proliferation and organization into nascent vascular structures are regulated by growth factor signaling through pathways involving FGF2, PDGF-BB, Ang-1, VEGFR-2 (KDR), and Tie-2.
5. Regulation of Vessel Size: Vessel maturation, stabilization, and permeability are controlled by endothelial adhesion molecules and signaling regulators such as VEGFR-1 (FLT1), ICAM-1, VCAM-1, E-selectin, P-selectin, vWF, and TGF-β isoforms.
6. Tumor Vascularization: Sustained angiogenesis within the tumor microenvironment is driven by inflammatory and immune-modulatory signals, including TNF-α, IL-6, IL-1β, GM-CSF, G-CSF, M-CSF, RANTES (CCL5), Galectin-9, S100A12, and CRP, supporting aberrant vascular growth and remodeling.

Angiogenesis is a multistep process defined by the following events:

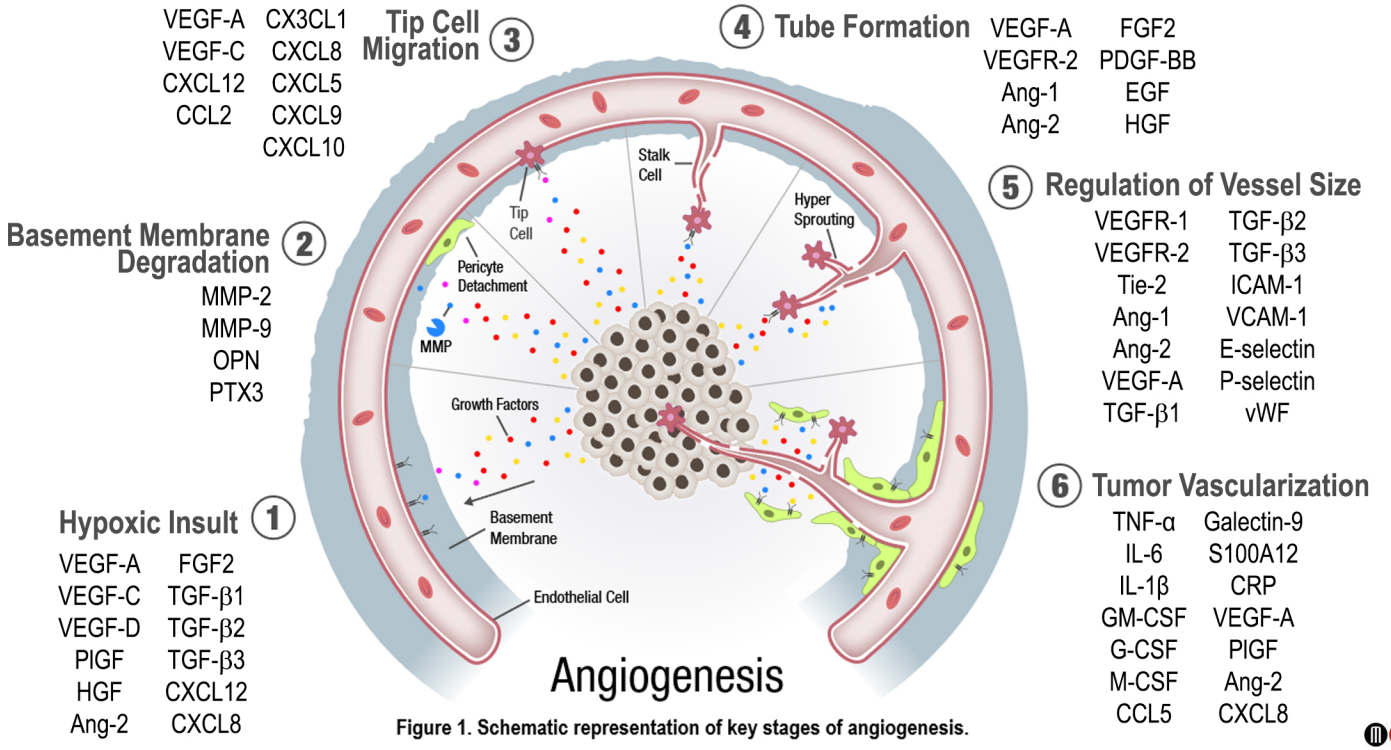

Figure 1. Schematic representation of key stages of angiogenesis.

Methods and Approach

Multiplex Assay Platform and Detection Technology

A 44-plex panel of circulating angiogenesis biomarkers ("Angiome panel") was assessed using the MESO SCALE DISCOVERY® (MSD) electrochemiluminescence (ECL) platform. Assays were configured on U-PLEX® plates, where linker-based capture chemistry enables flexible assembly of multiplex panels and grouping of analytes based on optimal sample dilution requirements (Figure 2 and Table 1).

All measurements were performed using <100 µL of plasma per sample, enabling efficient multiplex profiling across a broad dynamic range. TGF-β isoforms were quantified following a pre-analytical acid dissociation step to release latent complexes. All samples were assayed according to assay protocols as shown in Figure 2.

Assays were executed on the MESO® Parsec R 5000MM analyzer, ensuring standardized, high-throughput processing and reproducible assay performance. ECL signal detection provides high sensitivity and quantitative resolution across low- and high-abundance analytes.

Analytical Characterization and Validation

Analytical performance of the Angiome panel was evaluated using both recombinant protein controls and endogenous plasma samples to ensure accurate quantification across diverse analytes and concentration ranges.

- **Precision**:
  Intra- and inter-assay variability was assessed using quality controls and pooled plasma samples.
- **Accuracy and Recovery**:
  Spike and recovery experiments were performed on assays requiring less than 100-fold dilution using recombinant-protein spiked diluent and pooled human plasma.
- **Dilution Linearity**:
  Evaluated using four plasma samples at four dilutions.
- **Sensitivity and Dynamic Range**:
  Lower and upper limits of detection (LLOD, TOC) were established relative to observed biological concentrations.

Sample Sources and Study Design

Plasma samples were provided by Duke University from healthy volunteers and oncology cohort. Samples supported analytical validation, biological stability assessment, and translational pharmacodynamic analysis:

Healthy volunteer (longitudinal) cohort: Longitudinal plasma samples from 28 individuals (N=224 samples) were obtained from a previously characterized study (Liu, Cancer Epidemiol Biomarkers Prev, 2025). Data were analyzed using a mixed linear model to partition intra- and inter-individual variance. Intraclass correlation coefficients (ICC) were calculated using both unadjusted and covariate-adjusted models (age, sex, BMI, fasting status).

Oncology cohorts:

- **CaboMab study (NCT0047330)**: KRAS wt metastatic colorectal cancer treated with cabozantinib and panitumumab; baseline (n=27) and C2D1 (n=19).
- **XAG study (NCT02008383)**: metastatic esophagogastric cancer treated with oxaliplatin, capecitabine, and bevacizumab; baseline (n=49) and C4D1 (n=26).

Matched baseline and on-treatment plasma samples from oncology cohorts (CaboMab and XAG) were analyzed to assess therapy-induced modulation of circulating angiogenesis biomarkers.

For each analyte, changes from baseline were calculated within subjects and normalized using z-score transformation to enable cross-analyte comparison across differing concentration ranges.

Pharmacodynamic responses were visualized using heatmaps, where rows represent individual biomarkers and columns represent subjects. Color scaling reflects relative upregulation or downregulation from baseline, enabling identification of coordinated, pathway-level responses within and across cohorts.

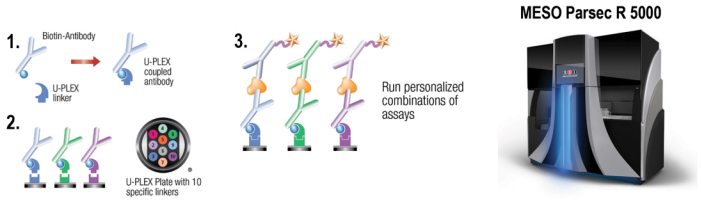

Figure 2. U-PLEX Technology: coupling, coating and assay workflow on the MESO Parsec R 5000. Biotinylated capture antibodies are conjugated to unique U-PLEX linkers (Step 1), enabling their directed immobilization onto predefined spots within each well of a U-PLEX plate (Step 2). Multiple linker–antibody conjugates are combined to generate a customized multiplex panel. Following sample incubation, analytes are captured and detected using SULFO-TAG™-labeled detection antibodies (Step 3), producing electrochemiluminescent signals proportional to analyte concentration. All assay steps, from plate coupling through signal detection and plate readout, were performed on the MESO Parsec 5000. This flexible configuration allows simultaneous, quantitative measurement of multiple targets from a single sample.

Table 1. Angiome 44-plex assays, characteristics, and dynamic range. Concentrations provided as dilution corrected values.

Biological Process	Gene ID	Protein Name	UniProt ID	Limit of Detection, pg/mL	Top of Curve, pg/mL
Hypoxic insult	CXCL8	Interleukin-8	P10145	0.2	1,900
	ANG2	Angiopoietin-2	O15123	7.8	140,000
	HGF	Hepatocyte growth factor	P14210	17	1,000,000
	PGF	Placental growth factor	P49763	1.0	2,500
	VEGFA	Vascular endothelial growth factor A	P15692	8.2	240,000
	VEGFC	Vascular endothelial growth factor C	P49767	20	160,000
	VEGFD	Vascular endothelial growth factor D	O43915	14	110,000
Basement membrane degradation	CDH1	E-cadherin	P12830	160	2,500,000
	DPP4	Dipeptidyl peptidase 4	P27487	23,000	88,000,000
	MMP2	Matrix metalloproteinase 2	P08253	2,400	2,300,000
	MMP9	Matrix metalloproteinase 9 (active)	P14780	8,400	2,000,000
	PTX3	Pentraxin 3	P26022	55	1,100,000
	SPP1	Osteopontin	P10451	50	3,200,000
Tip cell migration	CCL11	Eotaxin	P51671	2.6	100,000
	CCL2	Monocyte chemoattractant protein-1	P13500	13	24,800
	CX3CL1	Fractalkine	P78423	460	2,000,000
	CXCL10	Interferon gamma-induced protein 10	P02778	13	420,000
	CXCL12	Stromal cell-derived factor 1 alpha	P48061	1,300	320,000
	CXCL9	Monokine induced by IFN-γ	Q07325	0.8	32,800
Tube formation	ANG1	Angiopoietin-1	Q15389	390	16,000,000
	FGF2	Fibroblast growth factor 2	P09038	0.6	4,400
	FLT3L	FMS-like tyrosine kinase 3 ligand	P49771	13	140,000
	KDR	VEGF receptor 2	P35968	250	7,200,000
	PDGFB	Platelet-derived growth factor B	P01127	60	460,000
	TEK	TEK receptor tyrosine kinase	Q02763	230	2,600,000
Regulation of vessel size	FLT1	VEGF receptor 1	P17948	14	31,000
	ICAM1	Intercellular adhesion molecule 1	P05362	720	8,000,000
	SELE	E-selectin	P16581	1,600	3,200,000
	SELP	P-selectin	P16109	3,900	3,500,000
	TGFB1	Transforming growth factor beta 1	P01137	180	1,000,000
	TGFB2	Transforming growth factor beta 2	P61812	0.9	4,600
	TGFB3	Transforming growth factor beta 3	P10600	0.1	3,500
	VCAM1	Vascular cell adhesion molecule 1	P19320	6,000	96,000,000
	VWF	von Willebrand factor	P04275	60,000	4,000,000,000
Tumor vascularization	CCL5	CCL5	P13501	840	5,200,000
	CRP	C-reactive protein	P02741	2,700	27,000,000
	CSF1	Macrophage colony-stimulating factor	P09603	0.40	33,000
	CSF2	Granulocyte-macrophage colony-stimulating factor	P04141	0.10	4,000
	CSF3	Granulocyte colony-stimulating factor	P09919	0.19	3,600
	IL1B	Interleukin-1 beta	P01584	0.06	1,500
	IL6	Interleukin-6	P05231	0.05	1,400
	LGALS9	Galectin-9	O00182	29.0	560,000
	S100A12	Calgranulin C	P80511	720	12,000,000
	TNFA	Tumor necrosis factor alpha	P01375	0.17	1,900

Analytical Characterization, Performance and Validation

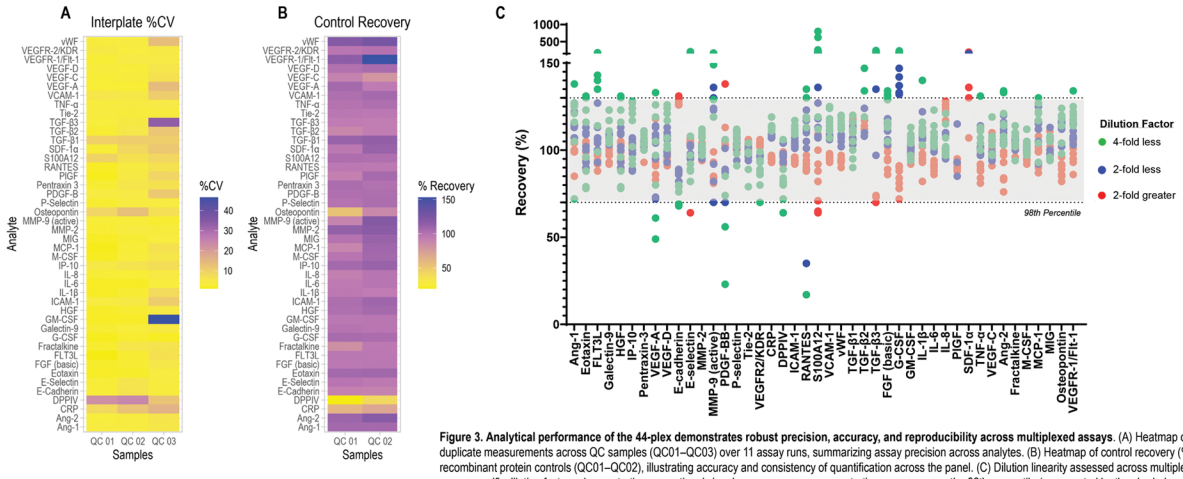

Figure 3. Analytical performance of the 44-plex demonstrates robust precision, accuracy, and reproducibility across multiplexed assays. (A) Heatmap of inter-plate %CV for duplicate measurements across QC samples (QC01–QC03) over 11 assay runs, summarizing assay precision across analytes. (B) Heatmap of control recovery (% recovery) for recombinant protein controls (QC01–QC02), illustrating accuracy and consistency of quantification across the panel. (C) Dilution linearity assessed across multiple plasma samples using assay-specific dilution factors, demonstrating proportional signal response across concentration ranges across the 98th percentile (represented by the shaded area). Across analytes, low inter-plate variability and consistent recovery profiles indicate reliable multiplex performance, while dilution linearity confirms quantitative accuracy across a broad dynamic range.

- High reproducibility (%CV <5% for 95% of analytes, recovery between 80-120% for 90% of analytes) across the Angiome enables confident comparison of biomarkers across samples and studies.
- When allowing ≥2 of 3 dilution levels to meet recovery criteria (≥75% samples within 70–140%), ~90% of assays demonstrated acceptable linearity, indicating robust performance across the usable dynamic range.
- Quantitative accuracy is maintained across diverse biomarker classes, supporting reliable measurement of both low- and high-abundance proteins.
- Consistent signal scaling across concentrations confirms that observed differences reflect true biological variation rather than assay artifacts.
- Robust performance in plasma matrices enables direct application to translational studies without loss of analytical fidelity.

Robust Angiome 44-plex Panel Performance Across Healthy and Cancer Plasma

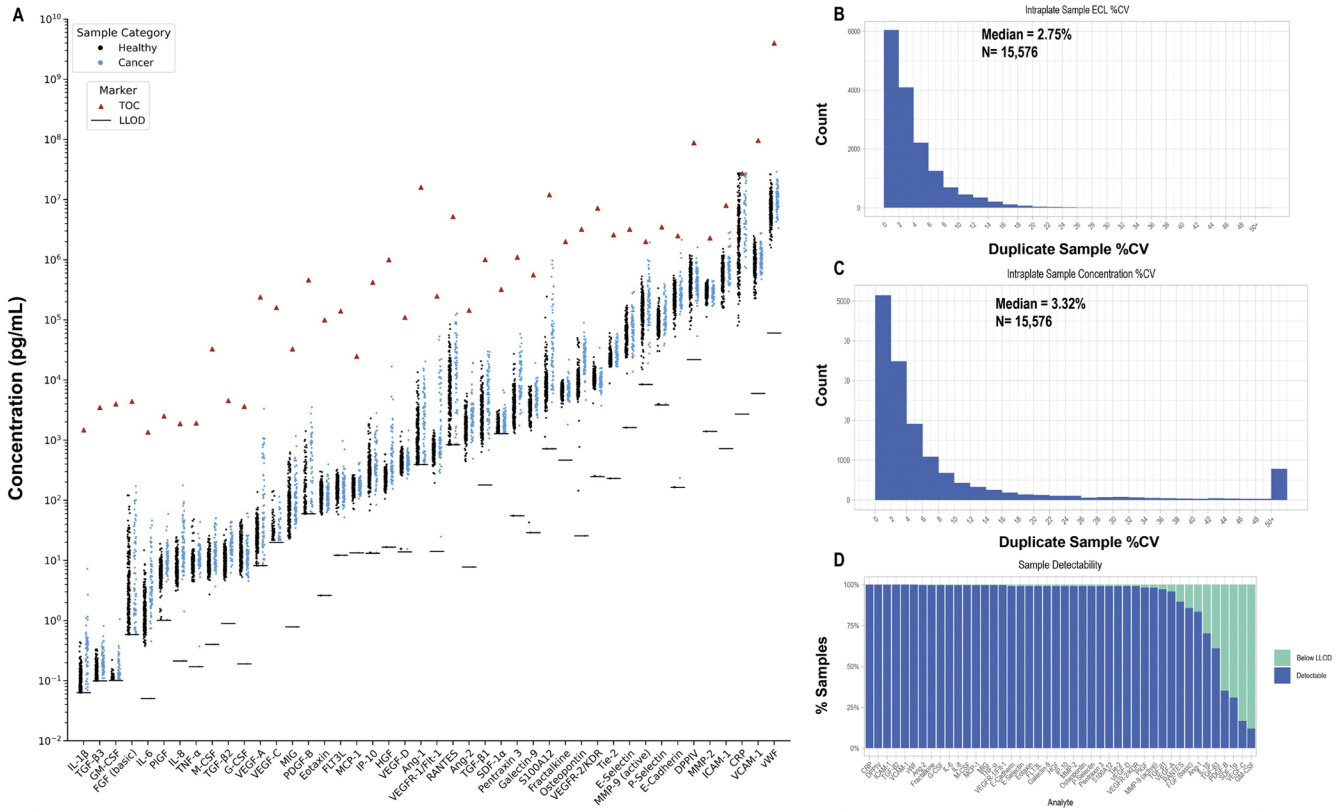

Figure 4. Analytical performance of the Angiome 44-plex panel across healthy and cancer plasma samples. (A) Concentration distributions for all analytes measured in duplicate across samples, with lower limits of detection (LLOD) and calibrator ranges (top of curve, TOC) indicated, demonstrating quantification across ~8–9 orders of magnitude. (B–C) Intra-plate precision assessed from duplicate measurements, showing tight reproducibility with median %CVs of 2.7% (ECL signal) and 3.3% (calculated concentration). (D) Percent detectability across analytes, with a median of ~80% across all samples.

Precision: Duplicate measurements demonstrate exceptional reproducibility across all analytes, with median %CVs of 2.7% (ECL) and 3.3% (concentration). This level of precision enables clear separation of biological signal from technical noise, supporting confident detection of subtle changes.

Dynamic Range: Using multiple sample dilutions and grouping assays by expected analyte abundance, the 44-plex workflow supports quantification across biomarkers spanning ~8–9 orders of magnitude in concentration.

Detectability: The panel achieves greater than 90% median detectability across healthy and cancer samples, ensuring consistent, biologically relevant coverage across heterogeneous sample populations and minimizing missing data that can confound downstream analyses.

Defining Stable and Dynamic Angiogenesis Biomarkers Using Interclass Coefficient Analysis and Longitudinal Profiling

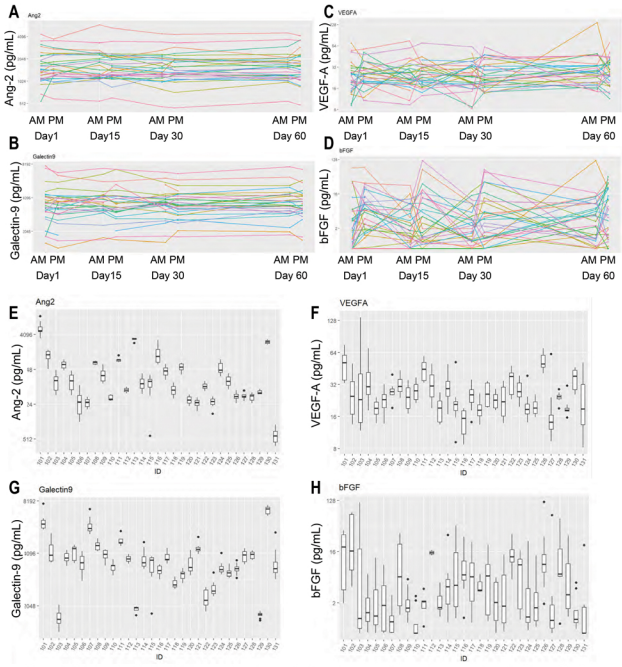

Figure 5. Distinct longitudinal behavior of angiogenesis biomarkers reveals stable versus dynamically regulated biology. (A–D) Spaghetti plots show individual longitudinal trajectories for Angiopoietin-2 (Ang-2), VEGF-A, Galectin-9 (Gal-9), and bFGF, respectively. (E–H) Corresponding boxplots summarize subject-level distributions across timepoints for each marker. Across markers, differences in trajectory, consistency, and distributional spread highlight varying degrees of longitudinal stability and intra-individual variability. Stable markers exhibit tightly clustered trajectories and minimal distributional shift over time, whereas more dynamic markers show increased dispersion and temporal fluctuation. These visual patterns align with adjusted ICC-derived stability metrics, supporting the distinction between consistently expressed biomarkers and those influenced by underlying physiological or temporal factors.

Table 2. Circulating angiogenesis markers exhibit a spectrum of biological stability, with select markers demonstrating high reproducibility across time while others reflect dynamic regulation

Biological Process	Assay	Median Range (pg/mL)	Unadjusted ICC	Adjusted ICC
Hypoxic insult	Ang-2	1,500 (440 – 5,900)	0.91 (0.85, 0.95)	0.90 (0.80, 0.95)
	VEGF-D	410 (260 – 1,400)	0.77 (0.65, 0.85)	0.84 (0.68, 0.91)
	PlGF	6.5 (1.0 – 19)	0.82 (0.71, 0.88)	0.77 (0.58, 0.87)
	HGF	240 (110 – 580)	0.68 (0.53, 0.78)	0.63 (0.39, 0.77)
	IL-8	6.7 (3.1 – 24)	0.66 (0.50, 0.77)	0.39 (0.16, 0.57)
	VEGF-A	25 (8.2 – 140)	0.38 (0.21, 0.53)	0.33 (0.12, 0.50)
	VEGF-C	20 (20 – 140)	0.30 (0.14, 0.44)	0.17 (0.012, 0.34)
Basement membrane degradation	E-Cadherin	220,000 (53,000 – 540,000)	0.86 (0.76, 0.91)	0.87 (0.74, 0.93)
	Osteopontin	8,800 (140 – 50,000)	0.55 (0.38, 0.68)	0.75 (0.56, 0.86)
	Pentraxin 3	3,600 (1,300 – 27,000)	0.77 (0.63, 0.85)	0.69 (0.46, 0.82)
	DPPIV	480,000 (70,000 – 1,200,000)	0.76 (0.64, 0.84)	0.69 (0.44, 0.81)
	MMP-2	300,000 (110,000 – 460,000)	0.59 (0.43, 0.71)	0.64 (0.41, 0.77)
	MMP-9 (active)	140,000 (8,400 – 530,000)	0.53 (0.35, 0.65)	0.47 (0.24, 0.65)
Tip cell migration	SDF-1α	1,300 (1,300 – 3,200)	0.77 (0.64, 0.85)	0.77 (0.58, 0.86)
	Fractalkine	6,900 (3,500 – 10,000)	0.72 (0.57, 0.81)	0.73 (0.51, 0.84)
	MIG	75 (23 – 630)	0.86 (0.76, 0.91)	0.70 (0.48, 0.82)
	Eotaxin	130 (57 – 300)	0.78 (0.66, 0.86)	0.66 (0.42, 0.79)
	MCP-1	170 (71 – 260)	0.60 (0.44, 0.72)	0.56 (0.30, 0.73)
	IP-10	300 (68 – 2,300)	0.75 (0.62, 0.83)	0.53 (0.29, 0.69)
Tube formation	Tie-2	22,000 (8,800 – 60,000)	0.82 (0.69, 0.88)	0.84 (0.68, 0.91)
	VEGFR-2/KDR	10,000 (4,100 – 24,000)	0.80 (0.68, 0.87)	0.78 (0.59, 0.87)
	FLT3L	150 (58 – 320)	0.61 (0.44, 0.73)	0.62 (0.36, 0.76)
	FGF (basic)	2.8 (0.6 – 120)	0.29 (0.13, 0.43)	0.31 (0.10, 0.49)
	PDGF-B	60 (60 – 1,400)	0.20 (0.072, 0.33)	0.16 (0.007, 0.33)
	Ang-1	1,000 (390 – 1,400)	0.15 (0.037, 0.27)	0.086 (0, 0.24)
Regulation of vessel size	VCAM-1	810,000 (230,000 – 2,500,000)	0.81 (0.69, 0.87)	0.76 (0.56, 0.86)
	vWF	7,100,000 (1,600,000 – 26,000,000)	0.80 (0.69, 0.87)	0.74 (0.54, 0.85)
	E-Selectin	58,000 (13,000 – 1700,00)	0.80 (0.67, 0.86)	0.72 (0.48, 0.84)
	TGF-β2	9.4 (4.6 – 33)	0.67 (0.50, 0.77)	0.70 (0.46, 0.82)
	ICAM-1	540,000 (160,000 – 1,500,000)	0.73 (0.59, 0.82)	0.66 (0.44, 0.80)
	TGF-β3	0.10 (0.10 – 0.30)	0.66 (0.50, 0.75)	0.64 (0.40, 0.77)
	P-Selectin	87,000 (30,000 – 330,000)	0.68 (0.52, 0.78)	0.58 (0.33, 0.72)
	VEGFR-1/Flt-1	670 (190 – 1,500)	0.55 (0.37, 0.67)	0.46 (0.23, 0.64)
	TGF-β1	2,600 (180 – 21,000)	0.15 (0.031, 0.28)	0.23 (0.048, 0.40)
Tumor vascularization	TNF-α	9.4 (4.5 – 48)	0.79 (0.66, 0.86)	0.78 (0.59, 0.87)
	Galectin-9	3,600 (1,400 – 7,900)	0.90 (0.83, 0.94)	0.76 (0.56, 0.86)
	M-CSF	8.5 (2.7 – 26)	0.77 (0.64, 0.85)	0.75 (0.54, 0.86)
	CRP	2,200,000 (80,000 – 27,000,000)	0.82 (0.71, 0.88)	0.73 (0.52, 0.83)
	G-CSF	13 (5.3 – 47)	0.74 (0.60, 0.83)	0.61 (0.38, 0.77)
	S100A12	8,000 (2,300 – 240,000)	0.42 (0.26, 0.56)	0.51 (0.28, 0.68)
	IL-1β	0.10 (0.10 – 0.40)	0.35 (0.19, 0.49)	0.41 (0.17, 0.59)
	IL-6	1.2 (0.40 – 15)	0.73 (0.59, 0.82)	0.40 (0.15, 0.59)
	GM-CSF	0.10 (0.10 – 0.20)	0.42 (0.25, 0.56)	0.15 (0.001, 0.31)
	RANTES	5,900 (840 – 84,000)	0.16 (0.045, 0.29)	0.12 (0, 0.26)

- Markers with high unadjusted ICC (e.g., Ang-2, VCAM-1, SDF-1α) demonstrate robust longitudinal stability, supporting their use for baseline stratification and cross-sectional comparisons without adjustment.
- Markers that increase upon covariate-adjusted ICC (e.g., ICAM-1, MIG, Eotaxin) reflect context-dependent regulation, indicating sensitivity to systemic physiological state and the need for controlled sampling or covariate-aware interpretation.
- Markers with consistently low ICC in both unadjusted and adjusted models (e.g., VEGF-A, VEGF-C, PDGF-B, Ang-1) exhibit true biological variability independent of covariates, consistent with active involvement in dynamic angiogenic processes and suitability as pharmacodynamic biomarkers.
- Together, integration of unadjusted and adjusted ICC defines a functional biomarker framework, distinguishing robust baseline markers, covariate-sensitive markers requiring contextual interpretation, and intrinsically dynamic markers that may capture drug-induced biological change.

Network-Level Pharmacodynamic Modulation of the Angiome

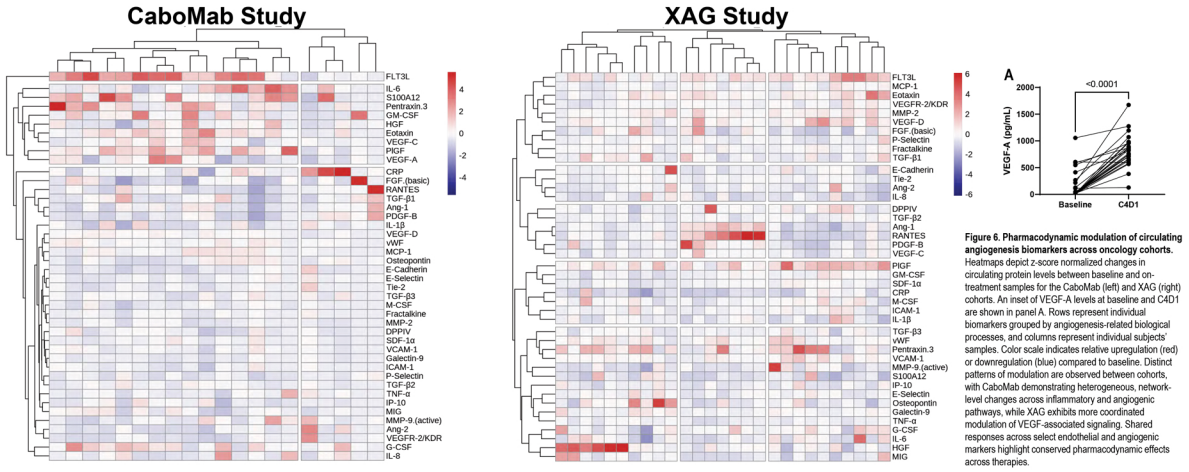

Figure 6. Pharmacodynamic modulation of circulating angiogenesis biomarkers across oncology cohorts. Heatmaps depict z-score normalized changes in circulating protein levels between baseline and on-treatment samples for the CaboMab (left) and XAG (right) cohorts. An inset of VEGF-A levels at baseline and C4D1 are shown in panel A. Rows represent individual biomarkers grouped by angiogenesis-related biological processes, and columns represent individual subjects' samples. Color scale indicates relative upregulation (red) or downregulation (blue) compared to baseline. Distinct patterns of modulation are observed between cohorts, with CaboMab demonstrating heterogeneous, network-level changes across inflammatory and angiogenic pathways, while XAG exhibits more coordinated modulation of VEGF-associated signaling. Shared responses across select endothelial and angiogenic markers highlight conserved pharmacodynamic effects across therapies.

- **Conserved vascular response:** Both regimens modulate core angiogenic pathways (VEGF/endothelial signaling), indicating shared pharmacodynamic effects on tumor vasculature.
- **Distinct response architectures:** CaboMab treatment exhibited a broad, immune-integrated remodeling signature, whereas XAG treatment exhibited a more focused, VEGF-axis–dominant response.
- **Therapy-specific biology:** These patterns highlight how different treatment mechanism shapes angiogenic network behavior—from diffuse, inflammation-linked signaling to coordinated vascular targeting.

Integrated Angiome Profiling Enables Translational Insight Into Vascular Biology and Tumor Angiogenesis

- A validated 44-plex platform delivers precise, high dynamic range quantification of angiogenesis biomarkers, supporting scalable profiling from discovery through translational research applications.
- Biomarker classification into stable and dynamic classes, combined with oncology cohort analysis, reveals therapy-specific angiogenic response architectures and supports baseline characterization and pharmacodynamic assessment.

DOWNLOAD POSTER